A Review On Retinal Blood Vessel Segmentation Methodologies

Aastha, Rahul Gautam

Abstract: Retinal blood vessel segmentation algorithms play a vital role for automatic screening of retinal diseases. It has a great impact in medical image analysis for early detection, treatment, and evaluation of cardiovascular and ophthalmologic diseases such as glaucoma, arteriosclerosis, diabetic retinopathy, hypertension and choroidal neovascularization by the clinician. Automatic retinal vessel segmentation technique helps the ophthalmologist to perform early screening and accomplish the treatment. This paper examines various blood vessel segmentation techniques on 2D retinal images captured from the fundus camera. The main aim of this paper is to review the challenges associated with retinal blood vessel segmentation, analyzing various segmentation methodologies such as pattern recognition techniques, model-based approaches, matched filtering, vessel tracing/tracking, mathematical morphology, multi-scale approaches, parallel/hardware-based approaches and giving a brief description on quantitative measures of performance for vessel segmentation as for example accuracy (Acc), true positive rate(TPR), false-positive rate(FPR), sensitivity(SN), specificity(SP) and area under receiver operating characteristic (ROC) curve. We aspire the reader a framework for the existing research; introducing a wide range of retinal vessel segmentation algorithms; discussing the current trends and future directions and summarizing the open problems. The performance of algorithms is compared on two publicly available databases (DRIVE and STARE).

Index Terms: Blood vessel segmentation, DRIVE database, hysteresis thresholding, image segmentation, mathematical morphology, medical imaging, retinal images, segmentation methodology.

1. INTRODUCTION

Retinal blood vessel segmentation plays a significant role in medical imaging. Delineation of morphological attributes of retinal blood vessel namely length, width, branch patterns, and angles are used in diagnosis, treatment, and evaluation of cardiovascular and ophthalmologic diseases such as glaucoma, diabetic retinopathy, arteriosclerosis, hypertension and choroidal neovascularization by the ophthalmologist[1]. As blindness is a terrifying problem, it a major concern for proper detection and analysis of vasculature which may further assist in the screening of diabetic retinopathy, exudates[2], hemorrhage [3], tortuosity[4], neovascularization[5], etc.Manual detection of diseases by the clinician is tedious, time-consuming and the probability of occurrence of errors increases which need the expertise to resolve, so as to avoid it automatic measurement is taken into account. In this paper we intend to focus on various segmentation techniques as for example pattern recognition techniques, model-based approaches, matched filtering, vessel tracing/tracking, mathematical morphology, multi-scale approaches, and parallel hardware-based approaches.The goal of this paper is to brief about existing segmentation algorithms and encompasses paper discussion in tabular form and summarizing the comparison of performance evaluation done for each category. Organization of the paper is as follows: (Section 2) discusses the material used for analysis, (Section 3) gives a discussion on performance metrics and (Section 4) gives a brief review on various existing segmentation techniques followed by conclusion in (Section 5).

- *Aastha is a student of Master of Technology in Computer Science and Engineering in Sant Longowal Institute of Engineering and Technology, Sangrur, Punjab, India. E-mail: aasthaharit@gmail.com*
- *Rahul Gautam is working as Assistant Professor in Computer Science and Engineering in Sant Longowal Institute of Engineering and Technology, Sangrur, Punjab, India. E-mail: rahulgautam@sliet.ac.in*

2 MATERIAL

Evaluation of retinal vessel segmentation techniques is carried out on publically available databases. Although there are many databases as an example Drive, Stare, Messidor, HRF, Review, Aria, ROC micro-aneurysm set, VICAVR, etc., our concerned analysis is done on Drive and Stare databases. Most of the techniques use either of the databases or uses both of them for assessing performance metrics.

2.1 DRIVE Database

The photographs were procured from a screening of diabetic retinopathy in Netherland. There are 40 images captured by Canon CR5 is a non-mydriatic camera with a field view of (FOV) 45 degree using 8 bits per color plane with a resolution of 768*584 pixels. It includes 2 sets; training set and the test set residing 20 images each. The test set comes with 20 ground truth images manually segmented by two experts and the training set containing 20 ground truth images manually segmented by only one expert, both with corresponding FOV mask images.

***Figure 1**. Retinal Image from DRIVE dataset*

2.2 STARE Database

The photographs were procured from a screening of diabetic retinopathy in Netherland. There are 40 images captured by Canon CR5 is a non-mydriatic camera with a field view of (FOV) 45 degree using 8 bits per color plane with a resolution

of 768*584 pixels. It includes 2 sets; training set and the test set residing 20 images each. The test set comes with 20 ground truth images manually segmented by two experts and the training set containing 20 ground truth images manually segmented by only one expert, both with corresponding FOV mask images.

Figure 2. *Retinal Image from STARE dataset*

3 PERFORMANCE METRICS

Performance evaluation holds a great impact on biomedical image segmentation. Basically, metrics demonstrate the comparison between proposed segmented image and ground truth image[6]. The conclusion of retinal vessel segmentation processes is pixel-based. The pixels can be classified either as a vessel or a non-vessel. Accordingly, four prospects are there; two classifications and two misclassifications. Further classification is categorized into two parts true positive (TP) and true negative (TN). In true positive, the pixel is determined into vessel both in-ground image and segmented image, whereas in the true negative pixel is identified as a non-vessel in both ground truth and segmented image. Same as with misclassification it is also divided into two parts false positive (FP) and false-negative (FN). In false positive, a pixel is classified as a vessel in the segmented image but a non-vessel ground truth and in a false-negative pixel is marked as a non-vessel in the segmented image but a vessel in ground truth image.Many other evaluation metrics are sensitivity (SN), specificity (SP), accuracy (ACC), PPV and npv. Sensitivity is also called a true positive rate (TPR), it measures truly detected vessel pixels whereas specificity measures truly classified non-vessels.

$$SN=TP/(TP+FN)$$

$$SN=TN/(TN+FP)$$

Accuracy is the ratio of total no of truly classified pixels to the FOV (field of view) pixel count [1]. PPV gives the probability that the classified pixel is a vessel pixel and NPV gives the probability that the classified pixel is a non-vessel. Other than this AUC gives the curve, also referred to as ROC (Receiver Operating Characteristic).

$$Acc=((TP+TN))/(FOV\ pixel\ count)$$

4 SEGMENTATION APPROACHES

There are numerous methods for retinal blood vessel segmentation such as pattern recognition techniques, model-based approaches, matched filtering, vessel tracing/tracking, mathematical morphology, multi-scale approaches, and parallel hardware-based approaches. Comparison table for performance evaluation of each individual is outlined at the end of each method which includes methodology, type of database used, sensitivity, specificity, accuracy, area under ROC. Also, a summarized table for categorization of retinal vessel segmentation method is also described briefly.

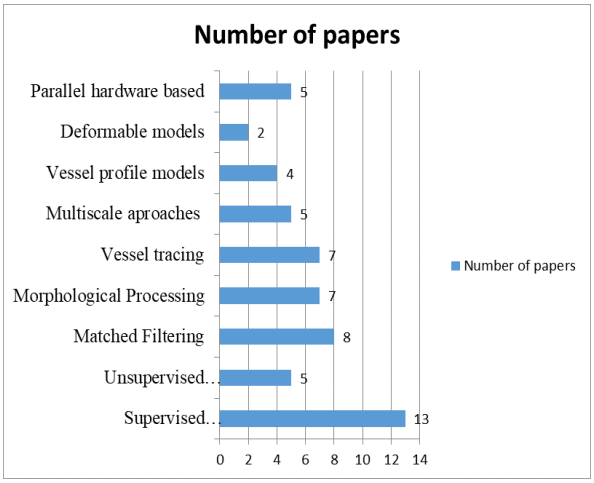

Figure 4. *Categorization of articles by retinal vessel segmentation techniques*

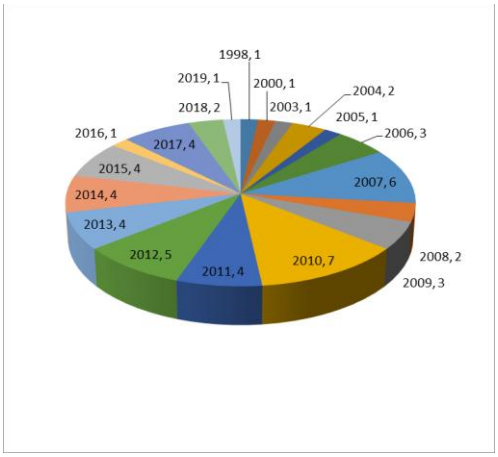

Figure 3. *Yearly analysis of reviewed articles*

***Table1**- Classification of retinal vessel segmentation methodologies*

Algorithm	Year	Image Processing Technique	Performance metrics	Nse/Pth/Cvr	Section
Staal et al [7]	2004	Image ridges and k-NN classifier	Acc, AUC	No	Supervised classification methods
Soares et al. [8]	2006	Gabor filter and Gaussian mixture model(GMM) classifier	Acc, AUC	No	
Ricci and Perfetti [9]	2007	Line operator and Support Vector Machine	Acc, AUC	Nse/Cvr	
Lupascu et al. [10]	2010	Feature-based AdaBoost classifier	SN, Acc, AUC	No	
Marin et al. [11]	2011	Gray level and moment invariant based features with neural network	SN, SP, Acc	Nse/Pth/Cvr	
Fraz et al. [12]	2011	Multi-scale Gabor filter and morphological transformation	SN, SP, Acc, AUC	No	
Fraz et al. [13]	2012	Ensemble classifier of bagged decision tress	SN,SP, Acc, AUC	Pth	
Wilfred and Edward. [14]	2014	ANN technique by Gabor and moment invariants-based features	Visual	Pth	
Wang et al. [15]	2015	Feature learning and ensemble classifier	SN, SP, Acc, AUC	No	
Vega et al. [16]	2015	Lattice Neural Networks with Dendritic processing	SN, SP, Acc	Nse	
Li et al. [17]	2016	Cross-modality learning approach	SN, SP, Acc	Nse/Pth	
Avijit and Sonam [18]	2017	A fully Convolutional Neural Network-based Structured Prediction	Acc, AUC	No	
Ren et al. [19]	2018	Feature learning	SN, SP, Acc	No	
Salem et al. [20]	2007	Radius based Clustering Algorithm (RACAL)	SN, SP	No	Unsupervised classification methods
Garg et al. [21]	2007	Curvature based	ROC, MAA	No	
Kande et al. [22]	2010	Spatially weighted fuzzy C-mean clustering	AUC	Pth/Nse	
Emary et al. [23]	2014	Possibilistic fuzzy c-means clustering	SN, SP, Acc	Nse/Pth	
Neto et al [24]	2017	Combination of Gaussian smoothening and morphological top-hat operator	SN, Acc	Cvr /Pth	
Hoover et al [25]	2000	MF and threshold probing	SN, SP, Acc	No	Matched Filtering
Xiaoyi and Monjon [26]	2003	Verification based multi-threshold probing	Acc, AUC	No	
Al-Rawi and Karajeh [27]	2007	Genetic algorithm matched filter optimization	Acc, AUC	No	
Chang et al. [28]	2007	Hessian-based filters and multiscale matched filters	SN, SP	No	
Cinsdikici and Aydin [29]	2009	Matched filter and ANT colony algorithm	SN, SP, Acc	No	
Zhang et al [30]	2010	Gaussian matched filter in combination with the first-order derivative	Acc, AUC	Pth	
Dehghani et al. [31]	2012	Histogram matching	Visual	Pth/Nse	
Chakraborti et al. [32]	2015	Self-adaptive matched filter	SN, SP, Acc	No	
Mendonca and Campilho [33]	2006	Combination of vessel centrelines and morphological reconstruction	Acc, AUC	No	Morphological procesing
Sekhar et al. [34]	2008	Hough Transform	Visual	No	
Miri and Mahloojifar [35]	2011	Curvelet transform and multi-structure elements morphology by reconstruction	TPR, FPR, Acc	Nse	
Fraz et al. [36]	2012	Vessel centerline detection and morphological bit-plane slicing	TPR, FPR, SN, SP, Acc, PPV	No	
Fraz et al. [37]	2013	Top-hat transformation and bit plane slicing	SN, SP, Acc	No	
Gour and Khanna [38]	2018	Hybrid median filtering and top-hat transformation	SN, SP, Acc		
Pal et al. [39]	2019	2D Wavelet transformation followed by CLAHE	SN, SP, Acc	Nse	
Chutatape et al. [40]	1998	Gaussian and Kalman filters	Visual	No	Vessel Tracing
Delibasis et al. [41]	2010	Model based tracing	SN, SP, Acc	No	
Adel et al. [42]	2010	Bayesian segmentation with MAP	Visual	No	
Kaul et al. [43]	2012	Minimal path-based algorithm	Visual	Nse	
Yin et al. [44]	2012	Probabilistic tracking method	ROC	No	
Bhuiyan et al. [45]	2013	Vessel edge tracking	Acc	Cvr/ Nse	
Chen et al. [46]	2014	Anisotropic minimal paths and Path score	Visual	No	
Li et al. [47]	2006	Gabor filter, scale multiplication, and adaptive thresholding	Visual	Nse	Multiscale approaches
Palomera-Perez et al. [48]	2010	Feature extraction and region growing	Visual	No	
Nguyen et al. [49]	2013	Multi-scale line detection	Acc	Cvr	
Sreejini and Govindan [50]	2015	Multiscale matched filter using PSO algorithm	SN, SP, Acc	Nse	
Elson et al. [51]	2017	SGO based MSMF	SN, SP, Acc	No	
Mahadevan et al. [52]	2004	Vessel profile model	Visual	Nse/Pth	Vessel profile models
T. Zhu [53]	2010	Fourier cross-sectional profile model	Visual	Nse/ Cvr	
Lazar and Hajdu [54]	2011	Rotating cross-section based model	Visual	Nse	
Lupascu et al. [55]	2013	Multiresolution Hermite model using ensembles of bagged decision trees	Visual	No	
Espona et al. [56]	2008	Snakes in combination with morphological processing	SN, SP, Acc	No	Deformable models
Zhang et al. [57]	2009	Nonlinear projections, variational calculus	TPR, FPR, Acc	No	
Alonso-Montes et al. [58]	2005	Cellular Neural network (CNN) based algorithm	Visual	No	Parallel hardware-based implementation
Perfetti et al. [59]	2007	CNN with virtual-template expansion	Acc, AUC	No	
Nieto et al. [60]	2009	Field Programmable Gate Arrays (FPGA) implementation	Visual	No	
Arguello et al. [61]	2014	GPU based	SN, SP, Acc	No	
Cavinato et al. [62]	2017	Software implementation and Hardware acceleration	SN, Acc	No	

4.1 Pattern recognition classification

Pattern recognition based segmentation techniques is mainly of two classes: supervised approach and unsupervised approach. In a supervised method, it uses specimen of trained data sets to classify an unknown pixel whether it is a pixel or no-pixel, whereas the unsupervised method does not require prior labeling of information for segmentation.

4.1.1 Supervised classification method

In a supervised method, it requires a trained dataset for training the learning model and also called a gold standard. The trained data set consist of manually segmented images. Anyhow, Staal et al. [7] describe a system for automated segmentation of 2-D retinal vessel colored images. A system builds on the extraction of image ridges that concur around the vessel centreline. Primitives are composed by ridges in the form of line elements. The line elements then help in partitioning the image into the patches by allocating each pixel to the closest line element. A local coordinate frame is defined by the line element within each patch. A kNN classifier is used for classifying feature vector. Performance evaluation is done on two publically available databases; STARE and Utrecht. The method gives 0.9516 of accuracy and 0.9614 of ROC curve on STARE database.Soares et al. [8] put forward a segmentation method using 2-D Gabor wavelet and supervised classification. Feature vectors incorporate pixels intensity and 2-D Gabor wavelet transform responses which are taken at multiple scales are used to represent each pixel. A Bayesian classifier is used to classify a pixel as a vessel or non-vessel. The methodology is tested on DRIVE and STARE databases achieving an average accuracy of 0.9466 and 0.9480 and the area under ROC as 0.9614 and 0.9671 respectively.The implementation of line operators and support vector classification is proposed by Ricci and Perfetti [9]. A line detector is used on green channels of retinal images. The developed image is thresholded to acquire unsupervised classification of a binary pixel. For more improvement, a supervised method is proposed to compute feature vector where linear SVM (support vector machine) is used as a classifier. DRIVE and STARE databases are used for assessing performance resulting in an average accuracy of 0.9563 and 0.9584 and the area under ROC curve as 0.9558 and 0.9602, respectively. Another method is proposed by Lupascu et al. [10] is Feature-based AdaBoost classifier (FABC). A 41-D feature vector is created for each pixel in the field of view (FOV) on geometry at multiple scales ($\sqrt{2}$, 2, $2\sqrt{2}$, and 4). The classifier is trained on 789 914 gold standard examples of vessels and non-vessels. The methodology is tested on the DRIVE database and achieves an average accuracy of 0.9597, an area under the ROC curve of 0.9561. Marin et al. [11] demonstrate a supervised segmentation method for a retinal vessel using a neural network determines a 7-D vector made up of grey-level and moment invariants-based features for representing a pixel. The result is formulated on DRIVE and STARE databases where the average accuracy, AUC, sensitivity and specificity is 0.9452, 0.9588, 0.7067, and 0.9801 on DRIVE database and 0.9526, 0.9769, 0.6944, and 0.9819 on STARE database, respectivelyFraz et al. [12] portray a supervised method for retinal vessel segmentation using line strength, multiscale Gabor and morphological features. By enumerating the outcomes of morphological linear operators, line strength and Gabor filters at multiple scales, a 7-D feature vector is a build which then encodes the spatial intensity. For classification of the retinal image into vessels and non-vessels, a Bayesian classifier and Gaussian mixture model is used. DRIVE and STARE databases are used for the evaluation of sensitivity are 0.7525 and 0.7604, specificity is 0.9722 and 0.9812, accuracy is 0.9476 and 0.9579 and area under ROC is 0.9616 and 0.9734, respectively. It performs better than the 2nd Human Observer. Another method proposed by Fraz et al. [13] uses ensemble system of bagged decision trees to utilize feature vector on the basis of the analysis of gradient vector filed, morphological transformation, line strength measures, and Gabor filter responses. The information is then encoded by the feature vector to handle both healthy and pathology in the retinal images. The results are carried out on DRIVE and STARE databases for which the sensitivity is 0.7406 and 0.7548, specificity is 0.9807 and 0.9763, accuracy is 0.9480 and 0.9534 and area under ROC is 0.9747 and 0.9768, respectively.Wilfred and Edward [14] bid a method employing ANN technique by Gabor and moment invariants-based features. In this, the use of multilayer perceptron neural network helps in identifying the retinal blood vessels and the inputs are derived from Gabor and moment invariants-based features. The backpropagation algorithm is also utilized in this work for changing weights in a feed-forward network. Feature learning and ensemble classifier based segmentation method is proposed by Wang et al. [15]. In this Convolutional neural network (CNN) and Random forest (RF) classifiers are combined together, where CNN extracts a hierarchical set of features and trained RF for vessel classification. It results in achieving sensitivity/specificity/accuracy/area under ROC for DRIVE database is 0.8173/0.9733/0.9767/0.9475 and for STARE database is 0.8104/0.9791/0.9813/0.9751. Vega et al. [16] put forward his work using Lattice neural network with dendritic processing(LNNDP). It does not require any parameter, rather it automatically builds its structure for solving the problem. The Hotelling T^2 is used in a post-processing step to decrease the 7-D feature vector to 5-D. The computations are performed on DRIVE and STARE databases and give sensitivity 0.7444 and 0.7019, specificity 0.9600 and 0.9671 and accuracy 0.9412 and 0.9483, respectively. Li et al [17] propound a cross-modality learning approach for retinal vessel segmentation. This work utilizes a deep neural network to replica the relation between the retinal image and the vessel map. It outperforms results on DRIVE and the STARE databases in terms of sensitivity is 0.7569 and 0.7726, specificity is 0.9816 and 0.9844, accuracy is 0.9527 and 0.9628 and area under ROC is 0.9738 and 0.9879, respectively. Avijit and Sonam [18] proposed a model using fully Convolutional neural network(CNN) based on structure prediction. Vessel segmentation problem is constructed as multi-label inference and use the advantage of combining CNN and structured prediction. It performs the evaluation on DRIVE database evolving sensitivity of 0.7691, the specificity of 0.9801, accuracy of 0.9533 and area under ROC is 0.9744. The supervised feature learning method is presented by Ren et al. [19]. It first selects the patches from grayscale retinal images and is treated as trained data. Then it combines the benefits of generalized low-rank approximations of matrices (GLRAM) and supervised manifold regularization (SMR) to learn new features. The learned features are the vectorized and are used to train the support vector machine (SVM) classifier. SVM classifier then classifies the pixels in a test image as drusen or non-drusen. The performance evaluation

is done on DRIVE and STARE databases giving 0.8741 and 0.9003 of sensitivity, 0.9493 and 0.9706 of specificity and 0.9481 and 0.9692 of accuracy, respectively.

***Table 2**- Performance measure for supervised methods*

Methodology	Database	Sensitivity	Specificity	Accuracy	Area under ROC
Staal et al. [7]	DRIVE	-	-	0.9442	0.952
	STARE	-	-	0.9516	0.9614
Soares et al. [8]	DRIVE	-	-	0.9466	0.9614
	STARE	-	-	0.9480	0.9671
Ricci and Perfetti [9]	DRIVE	-	-	0.9563	0.9558
	STARE	-	-	0.9584	0.9602
Lupascu et al. [10]	DRIVE	0.72	-	0.9597	0.9561
Marin et al. [11]	DRIVE	0.7067	0.9801	0.9452	0.9588
	STARE	0.6994	0.9819	0.9526	0.9769
Fraz et al. [12]	DRIVE	0.7525	0.9722	0.9476	0.9616
	STARE	0.7604	0.9812	0.9579	0.9734
Fraz et al. [13]	DRIVE	0.7406	0.9807	0.9480	0.9747
	STARE	0.7548	0.9763	0.9534	0.9768
Wang et al. [15]	DRIVE	0.8173	0.9733	0.9767	0.9475
	STARE	0.8104	0.9791	0.9813	0.9751
Vega et al. [16]	DRIVE	0.7444	0.9600	0.9412	-
	STARE	0.7019	0.9671	0.9483	-
Li et al. [17]	DRIVE	0.7569	0.9816	0.9527	0.9738
	STARE	0.7726	0.9844	0.9628	0.9879
Avijit and Sonam [18]	DRIVE	0.7691	0.9801	0.9533	0.9744
Ren et al. [19]	DRIVE	87.41%	94.93%	94.81%	-
	STARE	90.03%	97.06%	96.92%	-

4.1.2 Unsupervised classification method

In an unsupervised approach, there is an absence of prior labeling and trained data set. Salem et al. [20] proposed an unsupervised RAdius based Clustering Algorithm(RACAL) with partial supervision, and make use of distance-based principle to map the distribution of image pixels. To segment diameter of a small retinal vessel with low contrasts, the proposed work is enhanced by partial supervision. RACAL can also be used as a classifier for the automation process. The results are carried out on STARE database achieving a sensitivity of 0.8215 and specificity of 0.9750. Garg et al. [21] put forward his work utilizing curvature-based method to segment complete vessel tree for the retinal image. The vessels represent trenches and medial lines of trenches are extracted by the curvature. The absolute vessel tree is then extracted by the modified growing method. Performance is evaluated on the DRIVE database having accuracy 0.9361 and area under ROC 0.9271.Fuzzy based vessel segmentation in retinal images containing pathology is propounded by Kande et al. [22]. The method utilizes the intensity of red and green channel to rectify non-uniform illumination in the image. To intensify the contrast of retinal vessels against its background matched filtering is used and then they are segmented by making use of fuzzy c-means clustering-based thresholding. The results are carried out on DRIVE and STARE databases; accuracy is 0.8911 and 0.8976 and area under ROC is 0.9518 and 0.9298, respectively. Emary et al. [23] came up with possibilistic fuzzy c-means clustering(PFCM) to overcome fuzzy c-mean objective function. To achieve optimized clustering cuckoo search is used with PFCM. To handle the optimization of clustering, the cuckoo method is applied which is based on brood parasitic behavior of some cuckoo species with Levy flight behavior of some birds and fruit flies. The performance is analyzed on DRIVE and STARE databases with a sensitivity of 0.628 and 0.586, the specificity of 0.984 and 0.987 and accuracy of 0.938 and 0.94478, respectively.Neto et al [24] utilize a coarse-to-fine algorithm. To homogenize background and reduction of noise, a combination of Gaussian smoothening, top-hat operator and vessel contrast enhancement is employed. The statistics of spatial dependency and probability are used with an adaptive local threshold to coarsely estimate the vessel map. Then the segmentation is filtered through analysis of curvature and morphological reconstruction, reducing mislabelling of pixels and better estimation of retinal vessel tree. The proposed approach handles mislabelling of central vessel reflex regions and pathology in the retinal images. The outcome is evaluated on DRIVE and STARE databases where the sensitivity is 0.7806 and 0.8344, specificity is 0.9629 and 0.9443 and accuracy is 0.8718 and 0.8894, respectively.

***Table 3**- Performance measure for unsupervised methods*

Methodology	Database	Sensitivity	Specificity	Accuracy	Area under ROC
Salem et al. [20]	STARE	0.8215	0.9750	-	-
Garg et al. [21]	DRIVE	-	-	0.9361	0.9271
Kande et al. [22]	DRIVE	-	-	0.8911	0.9518
	STARE	-	-	0.8976	0.9298
Emary et al. [23]	DRIVE	0.628	0.984	0.938	-
	STARE	0.586	0.987	0.94478	-
Neto et al. [24]	DRIVE	0.7806	0.9629	0.8718	-
	STARE	0.8344	0.9443	0.8894	-

4.2 Matched filtering

Matched filters are acquired by associating a known signal with an unknown signal so as to detect the presence of shape in the unknown signal. Hoover et al. [25] proposed a matched filtering threshold probing approach to locate blood vessels and utilizes local and global vessel features collectively to perform vessel network segmentation. The evaluations are accomplished on hand-labeled segmented images, where the propound method decreases false positive by 15% and utmost 75% true positive rate over matched filtering response (MFR). Xiaoyi and Monjon [26] introduced to verification-based multi-threshold probing scheme, which generates hypotheses of objects provoked by binarization utilizing hypothetic threshold. And, hence the overall scheme is considered as knowledge-guide adaptive thresholding. The results are evaluated on the DRIVE database resulting in an accuracy of 0.9212 and area under ROC is 0.9114.Genetic algorithm matched filter optimization is put forward by Al-Rawi and Karajeh [27]. A new frame has been presented for sensitivity optimization under the proposed project, where the ROC is utilized as a fitness function. The estimated maximum average accuracy is

calculated to be 0.9420 and average area under ROC is 0.9582 on DRIVE database. Chang et al. [28] came up with a hybrid filtering approach to segment retinal vessel. The work is carried out by combining the Hessian matrix and matched filter response on multiple scales. For vessel inclination, Eigenvectors of a Hessian matrix are utilized. Edge constraints are employed to withhold the response of false boundary edges. The outcome is evaluated on the DRIVE database with the sensitivity of 0.95175 and specificity of 0.90234. Cinsdikici and Aydin [29] bid a hybrid model of matched filtering and ANT colony algorithm. The propound algorithm is adequate to extract retinal vessels and also helps in improving accuracy and false/true rates. The assessment of performance is carried out on the DRIVE database; measures accuracy of 0.9293 and area under ROC is 0.9407. Zhang et al. [30] proposed an extension of the matched filter(MF) approach, is a combination of MF and first-order derivative of Gaussian(FDOG). The thresholding to retinal image's response to MF helps to detect the vessels and the threshold is regulated by an image's response to the FDOG. The initiated work lessen the false observation of and detects more fine vessels left by MF. The performance is evaluated on DRIVE and STARE databases with a sensitivity of 0.7120 and 0.7177, a specificity of 0.9724 and 0.9753 and accuracy of 0.9382 and 0.9484, respectively.Histogram matching to localize optic disk in the presence of pathology is put forward by Dehghani et al. [31]. Many images are utilized to create templates. Rather than making an image as a template, three histograms are constructed with each one relating to only one color component. The mean histogram is evaluated as a template. Chakraborti et al. [32] came up with self-adaptive matched filtering by utilizing inclination histogram combines the vesselness filter with high sensitivity and matched filter with high specificity. The outcome is carried out on DRIVE and STARE databases achieving sensitivity 0.7205 and 0.6786, specificity 0.9579 and 0.9586 and accuracy 0.9370 and 0.9379, respectively.

Table 4*-Performance measure based on Matched filtering*

Methodology	Database	Sensitivity	Specificity	Accuracy	Area under ROC
Hover et al. [25]	STARE	0.6751	0.9567	0.9267	-
Xiaoyi and Mojon [26]	DRIVE	-	-	0.9212	0.9114
	STARE	-	-	0.9337	0.8906
Al-Rawi and Karajeh [27]	DRIVE	-	-	0.9420	0.9582
Chang et al. [28]	DRIVE	0.95175	0.90234	-	-
Cinsdikici and Aydin [29]	DRIVE	-	-	0.9293	0.9407
Zhang et al. [30]	DRIVE	0.7120	0.9724	0.9382	-
	STARE	0.7177	0.9753	0.9484	-
Chakraborti et al. [32]	DRIVE	0.7205	0.9579	0.9370	-
	STARE	0.6786	0.9586	0.9379	-

4.3 Morphological processing

Morphology is a branch of biology that dealt with forms and shapes of plants and animals. Morphological operators are mainly concerned with binary images however they can be outstretched to grey level images. Mendonca and Campilho [33] describes the combination of centrelines and morphological reconstruction. The vessel centrelines are extracted for vessel filling phase for which it provides the suggestions, where the four differential operators are handled to choose the set of candidate points which are then classified as centreline pixels. And ultimately the iterative region growing method is used for further classification. The evaluation is measured on DRIVE and STARE databases for which the sensitivity is 0.7334 and 0.6996, specificity is 0.9764 and 0.9730 and the accuracy is 0.9452 and 0.9440, respectively. Sekhar et al. [34] proposed a Hough transformation strategy to localize retinal optic disk. Morphological processing leads to establish the circular region and then Hough transform is utilized to observe circular feature in a positive horizontal gradient within the same interest. Curvelet transforms and multi-structure elements morphology by reconstruction is propounded by Miri and Mahloojifar [35]. Multi structure elements are used to detect ridges in the retinal image. Reconstruction banishes those ridges that do not belong to the vessels. Combination of the threshold with connected component analysis (CCA) identifies the ridges that belong to vessels. Performance evaluation is carried out on DRIVE database where the sensitivity is 0.7352, specificity is 0.9795 and accuracy is 0.9458.Fraz et al. [36] proposed a bit-planes slicing and centreline detection technique. Blood vessel framework is achieved by recognizing vessel centrelines and its shape where the orientation map is processed by bit-planes slicing. Centrelines and maps are combined together to segment vessel tree. The implementation is measured on DRIVE and STARE databases; sensitivity is 0.7152 and 0.7311, specificity is 0.9768 and 0.968054 and accuracy is 0.9430 and 0.9442, respectively. Another approach propound by Fraz et al. [37] describes a combination of top-hat transform and bit plane slicing strategy. The vessels are extracted by applying differential operator and the top-hat transform operator highlight distinct vessel direction and the information is gathered by bit-plane slicing. The method is tested on DRIVE and STARE databases with a sensitivity of 0.7302 and 0.7318, specificity is 0.9742 and 0.9660 with an accuracy of 0.9422 and 0.9423, respectively.Hybrid median filtering and top-hat transformation are carried out by Gour and Khanna [38]. The hybrid median filter keeps the narrow lines, protecting the corners. The results are evaluated on DRIVE and STARE databases; sensitivity is 0.7215 and 0.7405, specificity is 0.9729 and 0.9649 and the accuracy is 0.9409 and 0.9369, respectively. Pal et al. [39] presented 2D wavelet transformation followed by CLAHE to preprocess low contrast images. To separate retinal vessels from the background, a combination of hit-or-miss transform and the multi-structure element is utilized. Hysteresis thresholding is then accomplished to eliminate the undesirable areas from the binary image. Performance is measured on DRIVE database with a sensitivity of 0.6129, specificity is 0.9744 and the accuracy is 0.9431.

Table 5*- Performance measure for Morphological processing*

Methodology	Database	Sensitivity	Specificity	Accuracy	Area under ROC
Mendonca and Campilho [33]	DRIVE	0.7334	0.9764	0.9452	-
	STARE	0.6996	0.9730	0.9440	-
Miri and Mahloojifar [35]	DRIVE	0.7352	0.9795	0.9458	-
Fraz et al.	DRIVE	0.7152	0.9768	0.9430	-

[36]					
	STARE	0.7311	0.968054	0.9442	-
Fraz et al. [37]	DRIVE	0.7302	0.9742	0.9422	-
	STARE	0.7318	0.9660	0.9423	-
Gour and Khanna [38]	DRIVE	0.7215	0.9729	0.9409	-
	STARE	0.7405	0.9649	0.9369	-
Pal et al. [39]	DRIVE	0.6129	0.9744	0.9431	-

4.4 Vessel tracing/tracking

Vessel tracing method is composed of seeds points that are accompanied by the growth process which is directed image-driven constraints. Chutatape et al. [40] proposed a vessel tracing method using Gaussian and Kalman filters, which engage in scanning and tracking. To locate the center and vessels cross-sectional profile, a Gaussian 2nd order derivative is utilized. An extended version of the Kalman filter is in practice to optimize the evaluation linearly. Delibasis et al. [41] bid a model-based tracing algorithm. The parametric model is used in the proposed algorithm and evaluates central axis and diameter of vessels, such that it actively bifurcate those vessels which aren't traced yet bypassing any interference. DRIVE database is used for performance evaluation. The statistical-based tracking method is described by Adel et al. [42]. The propound work undergoes is connected with Maximum a posteriori (MAP) to detect edges. Kaul et al. [43] presented a minimal path algorithm to detect curves both open and closed without necessitating any preceding knowledge. The work is tested on 48 images in opposition to ground truth images. Yin et al [44] proposed a probabilistic tracking method to detect retinal blood vessel. Edge points are observed by applying local grey level statistics and preceding information. Confined vessels are evaluated by Gaussian curve and Bayesian with MAP, also discovers the edge points. Bhuiyan et al. [45] describes an edge-based vessel tracking method and calculates the width of the vessel to quantify Central Retinal Artery Equivalent (CRAE) and Central Retinal Vein Equivalent (CRVE). Another approach proposed by Chen et al. [46] utilizing anisotropic minimal paths and path scores for vessel extraction evaluated by optimally oriented flux centreline map (OOFCM). The proposed method is an extension of curve length measured anisotropic path scores.

4.5 Multi-scale approaches

Multi-scale approaches outperform readily at the alternate resolution of an image with an escalated processing speed, where the large vessels are bifurcated from low resolution and fine vessels from high resolution. Li et al. [47] put forward a multi-scale approach utilizing Gabor filter and Scale multiplication. The proposed work combines adaptive thresholding and multi-scaling, so as to help the ophthalmologist in diagnosis and screening programs which as suitable for detecting both small and large vessels simultaneously and also handles noise in the input images efficiently. Palomera-Perez et al. [48] present multi-scale feature extraction and region growing method, executing on parallel bifurcation and registration toolkit. The propound method results in much faster segmentation in high-resolution images.Nguyen et al. [49] proposed line detection for multi-scaling retina; vessel segmentation. The multi-scale line detectors are attained by simply changing the length of the primary line detector. The responses of multi-scale line detector are linearly merged to bifurcate the retinal blood vessels. The presented work handles the central reflex vessels in the retinal images and the performance is measured on DRIVE and STARE with an accuracy of 0.9407 and 0.9324, respectively. Sreejini and Govindan [50] presented a PSO algorithm and helps in suppressing the noise. To find a framework for optimal Gaussian filter, swarm optimization is utilized. The performance is evaluated on the DRIVE and STARE databases with a sensitivity of 71.32% and 71.72%, specificity is 98.66% and 96.87% and accuracy is 96.33% and 95.00%, respectively. Social group optimization (SGO) based multi-scale matched filtering (MSMF) is carried out by Elson et al. [51], is implemented in such a way to bear mining of retinal blood vessels. The images are procured from DRIVE and STARE databases. The statistical parameters are determined. The performance assesses the sensitivity of 0.7221 and 0.7307, the specificity of 0.9775 and 0.9635 with an accuracy of 0.9657 and 0.9528, respectively.

Table 6- *Performance measure for Multiscale approaches*

Methodology	Database	Sensitivity	Specificity	Accuracy	Area under ROC
Nguyen et al. [49]	DRIVE	-	-	0.9407	-
	STARE	-	-	0.9324	-
Sreejini and Govindan [50]	DRIVE	71.32%	98.66%	96.33%	-
	STARE	71.72%	96.87%	95.00%	-
Elson et al. [51]	DRIVE	0.7221	0.9775	0.9657	-
	STARE	0.7307	0.9635	0.9528	-

4.6 Model-based approaches

The model-based approach is classified into vessel profile models and deformable models. Vessel profile model concerns in strengthening the Gaussian shape where cubic spline and Hermite polynomial profile are switched, whereas the deformable model is further classified into a parametric deformable model and geometric deformable model.

4.6.1 Vessel profile model

Mahadevan et al [52] proposed a robust model to detect vessels in noisy images. The propound model is serviceable as nonlinear vessel improvement filter undergoing three steps; firstly testing the Huber's censored likelihood ration, then the second step is utilizing α-trimmed statistics and finally, the third step is for selecting robust model algorithm. The performance evaluation is carried out on phantom images. T. Zhu [53] presented a Fourier cross-sectional profile model with varying sharpness. The proposed scheme is unwavering as it employs phase congruency to evaluate symmetry and asymmetry in the Fourier domain. The work is also compared with Gaussian profile modeling and handles both noise and central vessel reflex in the retinal images. Lazar and Hajdu [54] describe a cross-section based model. Thresholding is utilized to construct microaneurysms (MA) score to obtain a probability score with high sensitivity and low positive rate. The proposed model does not require necessitate labeling. Lupascu et al. [55] present a multiresolution Hermite model using ensemble bagged decision trees. The proposed model results in better accuracies than REVIEW tests and Tayside tests, also the method is very much stable.

4.6.2 Deformable model

Espona et al. [56] proposed a deformable contour model, is a snake inspired by integrating topological properties. The propound work yields the automatic location of the optic disk and morphological segmentation. The results are carried out on the DRIVE database with a sensitivity of 0.7436, specificity is 0.9615 and accuracy is 0.9352. Nonlinear orthogonal projections for vessel detection is carried out by Zhang et al. [57]. Image decomposition model is implanted to scrutinize set of a concerned convex set. The performance is evaluated on DRIVE and STARE databases which measure the specificity of 0.9772 and 0.9736 and accuracy is 0.9610 and 0.9087, respectively.

***Table 7**- Performance measure for Model based approaches*

Methodology	Database	Sensitivity	Specificity	Accuracy	Area under ROC
Espona et al. [56]	DRIVE	0.7436	0.9615	0.9352	-
Zhang et al [57]	DRIVE		0.9772	0.9610	-
	STARE	0.7373	0.9736	0.9087	-

4.7 Parallel hardware-based implementation

Parallel hardware is implemented on VLSI chips where there is a need for real-time computation which utilizes segmentation and registration ToolKit. Alonso-Montes et al. [58] proposed a cellular neural network aiming to attain real-time prerequisite. The described work is performed on 3×3 CNN chipsets which are based on CNNUM prototype. CNN with the virtual-template expansion is described by Perfetti et al. [59], is based on linear space-invariant. The proposed work is carried out on ACE16K template and the performance is measured on the DRIVE database with an accuracy of 0.9348 and Area under ROC is 0.9261.Nieto et al. [60] presented a FPGA implementation for vessel extraction, an application-oriented scheme utilizes SIMD architecture which is portrayed on Spartan 3. The chipset evolved is of 1.4Mb and preserves 8 grey images of 144×160px. Arguello et al. [61] describes a GPU based bifurcation algorithm and incorporates a hybrid strategy by combining global image filters and contour tracing. The proposed work is evaluated on DRIVE and STARE databases with the sensitivity of 0.7209 and 0.7305, specificity is 0.9758 and 0.9688 and accuracy is 0.9431 and 0.9448, respectively. Cavinato et al. [62] propound software implementation and hardware acceleration. Field Programmable Gate Arrays (FPGA) is utilized either partially or entirely, aiming to outperform vessel bifurcation. The results are measured on DRIVE and STARE databases with a sensitivity of 0.6457 and 0.7291 and an accuracy of 0.9293 and 0.9030, respectively.

***Table8-** Performance measure for Parallel hardware based approaches*

Methodology	Database	Sensitivity	Specificity	Accuracy	Area under ROC
Perfetti et al. [59]	DRIVE			0.9348	0.9261
Arguello et al. [61]	DRIVE	0.7209	0.9758	0.9431	-
	STARE	0.7305	0.9688	0.9448	-
Cavinato et al. [62]	DRIVE	0.6475	-	0.9293	
	STARE	0.7291	-	0.9030	-

5 CONCLUSION

As for now, the extraction of the vasculature from the fundus images and has led to a wide research area. The scrupulous result of segmentation is mandatory for retinal vessel screening and identification of the disorders by an ophthalmologist. The main motive of this paper is to introduce various retinal segmentation techniques and how we can measure performance on the varied publically available database as per choice. Although many promising retinal vessel segmentation techniques have been developed even then much more improvement can be done on retinal vessel segmentation methodologies as the future of segmentation analysis is concerned in developing automated and accurate techniques.

REFERENCES

[1] M. M. Fraz et al., “Blood vessel segmentation methodologies in retinal images – A survey,” Comput. Methods Programs Biomed., vol. 108, no. 1, pp. 407–433, Oct. 2012.

[2] D. Youssef and N. H. Solouma, “Accurate detection of blood vessels improves the detection of exudates in color fundus images,” Comput. Methods Programs Biomed., vol. 108, no. 3, pp. 1052–1061, Dec. 2012.

[3] P. Jitpakdee, P. Aimmanee, and B. Uyyanonvara, “A survey on hemorrhage detection in diabetic retinopathy retinal images,” in 2012 9th International Conference on Electrical Engineering/Electronics, Computer, Telecommunications and Information Technology, 2012, pp. 1–4.

[4] A. Bhuiyan, B. Nath, K. Ramamohanarao, R. Kawasaki, and T. Y. Wong, “Automated Analysis of Retinal Vascular Tortuosity on Color Retinal Images,” J. Med. Syst., vol. 36, no. 2, pp. 689–697, Apr. 2012.

[5] S. S. A. Hassan, D. B. L. Bong, and M. Premsenthil, “Detection of Neovascularization in Diabetic Retinopathy,” J. Digit. Imaging, vol. 25, no. 3, pp. 437–444, Jun. 2012.

[6] N. Singh and L. Kaur, “A survey on blood vessel segmentation methods in retinal images,” 2015 Int. Conf. Electron. Des. Comput. Networks Autom. Verif. EDCAV 2015, pp. 23–28, 2015.

[7] J. Staal, M. D. Abramoff, M. Niemeijer, M. A. Viergever, and B. van Ginneken, “Ridge-Based Vessel Segmentation in Color Images of the Retina,” IEEE Trans. Med. Imaging, vol. 23, no. 4, pp. 501–509, Apr. 2004.

[8] J. V. B. Soares, J. J. G. Leandro, R. M. Cesar, H. F. Jelinek, and M. J. Cree, “Retinal vessel segmentation using the 2-D Gabor wavelet and supervised classification,” IEEE Trans. Med. Imaging, vol. 25, no. 9, pp. 1214–1222, Sep. 2006.

[9] E. Ricci and R. Perfetti, “Retinal Blood Vessel Segmentation Using Line Operators and Support Vector Classification,” IEEE Trans. Med. Imaging, vol. 26, no. 10, pp. 1357–1365, Oct. 2007.

[10] C. A. Lupascu, D. Tegolo, and E. Trucco, “FABC: Retinal Vessel Segmentation Using AdaBoost,” IEEE Trans. Inf. Technol. Biomed., vol. 14, no. 5, pp. 1267–1274, Sep. 2010.

[11] D. Marín, A. Aquino, M. E. Gegundez-Arias, and J. M. Bravo, “A New Supervised Method for Blood Vessel Segmentation in Retinal Images by Using Gray-Level

and Moment Invariants-Based Features," IEEE Trans. Med. Imaging, vol. 30, no. 1, pp. 146–158, Jan. 2011.

[12] M. M. Fraz, P. Remagnino, A. Hoppe, S. Velastin, B. Uyyanonvara, and S. A. Barman, "A supervised method for retinal blood vessel segmentation using line strength, multiscale Gabor and morphological features," in 2011 IEEE International Conference on Signal and Image Processing Applications (ICSIPA), 2011, pp. 410–415.

[13] M. M. Fraz et al., "An Ensemble Classification-Based Approach Applied to Retinal Blood Vessel Segmentation," IEEE Trans. Biomed. Eng., vol. 59, no. 9, pp. 2538–2548, Sep. 2012.

[14] S. W. Franklin and S. E. Rajan, "Retinal vessel segmentation employing ANN technique by Gabor and moment invariants-based features," Appl. Soft Comput., vol. 22, pp. 94–100, Sep. 2014.

[15] S. Wang, Y. Yin, G. Cao, B. Wei, Y. Zheng, and G. Yang, "Hierarchical retinal blood vessel segmentation based on feature and ensemble learning," Neurocomputing, vol. 149, no. PB, pp. 708–717, Feb. 2015.

[16] R. Vega, G. Sanchez-Ante, L. E. Falcon-Morales, H. Sossa, and E. Guevara, "Retinal vessel extraction using Lattice Neural Networks with dendritic processing," Comput. Biol. Med., vol. 58, pp. 20–30, Mar. 2015.

[17] Q. Li, B. Feng, L. Xie, P. Liang, H. Zhang, and T. Wang, "A Cross-Modality Learning Approach for Vessel Segmentation in Retinal Images," IEEE Trans. Med. Imaging, vol. 35, no. 1, pp. 109–118, Jan. 2016.

[18] A. Dasgupta and S. Singh, "A fully convolutional neural network based structured prediction approach towards the retinal vessel segmentation," in 2017 IEEE 14th International Symposium on Biomedical Imaging (ISBI 2017), 2017, pp. 248–251.

[19] X. Ren et al., "Drusen Segmentation From Retinal Images via Supervised Feature Learning," IEEE Access, vol. 6, pp. 2952–2961, 2018.

[20] S. A. Salem, N. M. Salem, and A. K. Nandi, "Segmentation of retinal blood vessels using a novel clustering algorithm (RACAL) with a partial supervision strategy," Med. Biol. Eng. Comput., vol. 45, no. 3, pp. 261–273, Feb. 2007.

[21] S. Garg, J. Sivaswamy, and S. Chandra, "Unsupervised curvature-based retinal vessel segmentation," in 2007 4th IEEE International Symposium on Biomedical Imaging: From Nano to Macro, 2007, pp. 344–347.

[22] G. B. Kande, P. V. Subbaiah, and T. S. Savithri, "Unsupervised Fuzzy Based Vessel Segmentation In Pathological Digital Fundus Images," J. Med. Syst., vol. 34, no. 5, pp. 849–858, Oct. 2010.

[23] E. Emary, H. M. Zawbaa, A. E. Hassanien, G. Schaefer, and A. T. Azar, "Retinal vessel segmentation based on possibilistic fuzzy c-means clustering optimised with cuckoo search," in 2014 International Joint Conference on Neural Networks (IJCNN), 2014, pp. 1792–1796.

[24] L. Câmara Neto, G. L. B. Ramalho, J. F. S. Rocha Neto, R. M. S. Veras, and F. N. S. Medeiros, "An unsupervised coarse-to-fine algorithm for blood vessel segmentation in fundus images," Expert Syst. Appl., vol. 78, pp. 182–192, Jul. 2017.

[25] A. Hoover, V. Kouznetsova, and M. Goldbaum, "Locating blood vessels in retinal images by piecewise threshold probing of a matched filter response," IEEE Trans. Med. Imaging, vol. 19, no. 3, pp. 203–210, Mar. 2000.

[26] Xiaoyi Jiang and D. Mojon, "Adaptive local thresholding by verification-based multithreshold probing with application to vessel detection in retinal images," IEEE Trans. Pattern Anal. Mach. Intell., vol. 25, no. 1, pp. 131–137, Jan. 2003.

[27] M. Al-Rawi and H. Karajeh, "Genetic algorithm matched filter optimization for automated detection of blood vessels from digital retinal images," Comput. Methods Programs Biomed., vol. 87, no. 3, pp. 248–253, Sep. 2007.

[28] C. Wu, G. Agam, and P. Stanchev, "A HYBRID FILTERING APPROACH TO RETINAL VESSEL SEGMENTATION," in 2007 4th IEEE International Symposium on Biomedical Imaging: From Nano to Macro, 2007, pp. 604–607.

[29] M. G. Cinsdikici and D. Aydın, "Detection of blood vessels in ophthalmoscope images using MF/ant (matched filter/ant colony) algorithm," Comput. Methods Programs Biomed., vol. 96, no. 2, pp. 85–95, Nov. 2009.

[30] B. Zhang, L. Zhang, L. Zhang, and F. Karray, "Retinal vessel extraction by matched filter with first-order derivative of Gaussian," Comput. Biol. Med., vol. 40, no. 4, pp. 438–445, Apr. 2010.

[31] A. Dehghani, H. A. Moghaddam, and M.-S. Moin, "Optic disc localization in retinal images using histogram matching," EURASIP J. Image Video Process., vol. 2012, no. 1, p. 19, Dec. 2012.

[32] T. Chakraborti, D. K. Jha, A. S. Chowdhury, and X. Jiang, "A self-adaptive matched filter for retinal blood vessel detection," Mach. Vis. Appl., vol. 26, no. 1, pp. 55–68, Jan. 2015.

[33] A. M. Mendonca and A. Campilho, "Segmentation of retinal blood vessels by combining the detection of centerlines and morphological reconstruction," IEEE Trans. Med. Imaging, vol. 25, no. 9, pp. 1200–1213, Sep. 2006.

[34] S. Sekhar, W. Al-Nuaimy, and A. K. Nandi, "Automated localisation of retinal optic disk using Hough transform," in 2008 5th IEEE International Symposium on Biomedical Imaging: From Nano to Macro, 2008, pp. 1577–1580.

[35] M. S. Miri and A. Mahloojifar, "Retinal Image Analysis Using Curvelet Transform and Multistructure Elements Morphology by Reconstruction," IEEE Trans. Biomed. Eng., vol. 58, no. 5, pp. 1183–1192, May 2011.

[36] M. M. Fraz et al., "An approach to localize the retinal blood vessels using bit planes and centerline detection," Comput. Methods Programs Biomed., vol. 108, no. 2, pp. 600–616, Nov. 2012.

[37] M. M. Fraz, A. Basit, and S. A. Barman, "Application of Morphological Bit Planes in Retinal Blood Vessel Extraction," J. Digit. Imaging, vol. 26, no. 2, pp. 274–286, Apr. 2013.

[38] N. Gour and P. Khanna, "Blood Vessel Segmentation Using Hybrid Median Filtering and Morphological Transformation," in 2017 13th International Conference

on Signal-Image Technology & Internet-Based Systems (SITIS), 2017, vol. 2018-Janua, no. c, pp. 151–157.

[39] S. Pal, S. Chatterjee, D. Dey, and S. Munshi, “Morphological operations with iterative rotation of structuring elements for segmentation of retinal vessel structures,” Multidimens. Syst. Signal Process., vol. 30, no. 1, pp. 373–389, Jan. 2019.

[40] O. Chutatape, Liu Zheng, and S. M. Krishnan, “Retinal blood vessel detection and tracking by matched Gaussian and Kalman filters,” in Proceedings of the 20th Annual International Conference of the IEEE Engineering in Medicine and Biology Society. Vol.20 Biomedical Engineering Towards the Year 2000 and Beyond (Cat. No.98CH36286), 1998, vol. 6, no. 6, pp. 3144–3149.

[41] K. K. Delibasis, A. I. Kechriniotis, C. Tsonos, and N. Assimakis, “Automatic model-based tracing algorithm for vessel segmentation and diameter estimation,” Comput. Methods Programs Biomed., vol. 100, no. 2, pp. 108–122, Nov. 2010.

[42] M. Adel, A. Moussaoui, M. Rasigni, S. Bourennane, and L. Hamami, “Statistical-Based Tracking Technique for Linear Structures Detection: Application to Vessel Segmentation in Medical Images,” IEEE Signal Process. Lett., vol. 17, no. 6, pp. 555–558, Jun. 2010.

[43] V. Kaul, A. Yezzi, and Y. Tsai, “Detecting Curves with Unknown Endpoints and Arbitrary Topology Using Minimal Paths,” IEEE Trans. Pattern Anal. Mach. Intell., vol. 34, no. 10, pp. 1952–1965, Oct. 2012.

[44] Y. Yin, M. Adel, and S. Bourennane, “Retinal vessel segmentation using a probabilistic tracking method,” Pattern Recognit., vol. 45, no. 4, pp. 1235–1244, Apr. 2012.

[45] A. Bhuiyan, R. Kawasaki, E. Lamoureux, K. Ramamohanarao, and T. Y. Wong, “Retinal artery–vein caliber grading using color fundus imaging,” Comput. Methods Programs Biomed., vol. 111, no. 1, pp. 104–114, Jul. 2013.

[46] D. Chen, L. D. Cohen, and J.-M. Mirebeau, “Vessel extraction using anisotropic minimal paths and path score,” in 2014 IEEE International Conference on Image Processing (ICIP), 2014, no. 1, pp. 1570–1574.

[47] Q. Li, J. You, L. Zhang, and P. Bhattacharya, “A Multiscale Approach to Retinal Vessel Segmentation Using Gabor Filters and Scale Multiplication,” in 2006 IEEE International Conference on Systems, Man and Cybernetics, 2006, vol. 4, no. x, pp. 3521–3527.

[48] M. A. Palomera-Pérez, M. E. Martinez-Perez, H. Benítez-Pérez, and J. L. Ortega-Arjona, “Parallel multiscale feature extraction and region growing: Application in retinal blood vessel detection,” IEEE Trans. Inf. Technol. Biomed., vol. 14, no. 2, pp. 500–506, 2010.

[49] U. T. V. Nguyen, A. Bhuiyan, L. A. F. Park, and K. Ramamohanarao, “An effective retinal blood vessel segmentation method using multi-scale line detection,” Pattern Recognit., vol. 46, no. 3, pp. 703–715, Mar. 2013.

[50] K. S. Sreejini and V. K. Govindan, “Improved multiscale matched filter for retina vessel segmentation using PSO algorithm,” Egypt. Informatics J., vol. 16, no. 3, pp. 253–260, Nov. 2015.

[51] J. Elson, J. Precilla, P. Reshma, and N. S. Madhavaraja, “Automated extraction and analysis of retinal blood vessels with Multi Scale Matched Filter,” in 2017 International Conference on Intelligent Computing, Instrumentation and Control Technologies (ICICICT), 2017, vol. 2018-Janua, no. 1, pp. 775–779.

[52] V. Mahadevan, H. Narasimha-Iyer, B. Roysam, and H. L. Tanenbaum, “Robust Model-Based Vasculature Detection in Noisy Biomedical Images,” IEEE Trans. Inf. Technol. Biomed., vol. 8, no. 3, pp. 360–376, Sep. 2004.

[53] T. Zhu, “Fourier cross-sectional profile for vessel detection on retinal images,” Comput. Med. Imaging Graph., vol. 34, no. 3, pp. 203–212, Apr. 2010.

[54] I. Lazar and A. Hajdu, “Microaneurysm detection in retinal images using a rotating cross-section based model,” in 2011 IEEE International Symposium on Biomedical Imaging: From Nano to Macro, 2011, pp. 1405–1409.

[55] C. A. Lupaşcu, D. Tegolo, and E. Trucco, “Accurate estimation of retinal vessel width using bagged decision trees and an extended multiresolution Hermite model,” Med. Image Anal., vol. 17, no. 8, pp. 1164–1180, Dec. 2013.

[56] L. Espona, M. J. Carreira, M. G. Penedo, and M. Ortega, “Retinal vessel tree segmentation using a deformable contour model,” in 2008 19th International Conference on Pattern Recognition, 2008, pp. 1–4.

[57] Y. Zhang, W. Hsu, and M. L. Lee, “Detection of Retinal Blood Vessels Based on Nonlinear Projections,” J. Signal Process. Syst., vol. 55, no. 1–3, pp. 103–112, Apr. 2009.

[58] C. Alonso-Montes, D. L. Vilarino, and M. G. Penedo, “CNN-based Automatic Retinal Vascular Tree Extraction,” in 2005 9th International Workshop on Cellular Neural Networks and Their Applications, 2005, pp. 61–64.

[59] R. Perfetti, E. Ricci, D. Casali, and G. Costantini, “Cellular Neural Networks With Virtual Template Expansion for Retinal Vessel Segmentation,” IEEE Trans. Circuits Syst. II Express Briefs, vol. 54, no. 2, pp. 141–145, Feb. 2007.

[60] A. Nieto, V. M. Brea, and D. L. Vilarino, “FPGA-accelerated retinal vessel-tree extraction,” in 2009 International Conference on Field Programmable Logic and Applications, 2009, pp. 485–488.

[61] F. Argüello, D. L. Vilariño, D. B. Heras, and A. Nieto, “GPU-based segmentation of retinal blood vessels,” J. Real-Time Image Process., pp. 773–782, 2014.

[62] L. Cavinato, I. Fidone, M. Bacis, E. Del Sozzo, G. C. Durelli, and M. D. Santambrogio, “Software implementation and hardware acceleration of retinal vessel segmentation for diabetic retinopathy screening tests,” in 2017 39th Annual International Conference of the IEEE Engineering in Medicine and Biology Society (EMBC), 2017, pp. 1226–1229.